Optimal Charging Schedule for a Battery Switching Station Serving Electric Buses

Pengcheng You*, Student Member, IEEE*, Zaiyue Yang*, Member, IEEE*, Yongmin Zhang*, Student Member, IEEE*, Steven H. Low*, Fellow, IEEE*, and Youxian Sun

Abstract—We propose a model of a battery switching station (BSS) for electric buses (EBs) that captures the predictability of bus operation. We schedule battery charging in the BSS so that every EB arrives to find a battery ready for switching. We develop an efficient algorithm to compute an optimal schedule. It uses dual decomposition to decouple the charging decisions at different charging boxes so that independent subproblems can be solved in parallel at individual charging boxes, making the algorithm inherently scalable as the size of the BSS grows. We propose a direct projection method that solves these subproblems rapidly. Numerical results illustrate that the proposed approach is far more efficient and scalable than generic algorithms and existing solvers.

Index Terms—BSS, EB-to-charging-box assignment, dual decomposition, direct projection method.

I. Introduction

POWER system of the future will be more sustainable, promote extensive demand response, and support electric vehicles (EVs) and other distributed energy resources [1]. In particular, EV growth is both a challenge and an opportunity for the power grid as EVs are very large but flexible loads. Unregulated charging may add great stress to the distribution grid [2]; however, well-scheduled charging can provide great benefits, e.g., peak clipping and valley filling [3].

As a special form of EVs, electric buses (EBs) are gaining popularity [4]–[6]. The growth is particularly rapid where there is heavy government promotion as in China [7]–[9]. Unlike passenger cars, public transport such as EBs cannot park for a long time to charge their batteries. Battery switching is a more suitable approach that can switch the battery of an EB in a few

minutes. The unloaded batteries are then charged in the battery switching station (BSS). In [10], the economic feasibility of EBs in combination with BSSs has been verified. There is a growing literature on BSSs, e.g., [10]–[16]. In [11], a new business model for a microgrid-based BSS is put forward. An optimal dispatching strategy of a microgrid containing BSSs, wind generators, photovoltaic systems, fuel cells, micro turbines and diesel generators is given, considering battery and charger constraints. [12] proposes the use of batteries in a BSS as a countermeasure for surplus electricity from photovoltaics. [13] studies the impact of the location and size of a BSS on EV penetration and security of the distribution grid. Similarly, [14] describes a model for identifying the optimal geographic locations for BSSs and investigates how to best stage the roll-out of BSSs in Australia over an extended time period. Charging infrastructure for EVs is also developing fast to support the construction of BSSs, e.g., the functionality of a commercialized fast charger for a lithium-ion EV battery is presented in [15]. Since BSSs can operate as either an electrical load or an energy source, [16] analyses the behavior of an Autonomous Power System (APS) with a high penetration of generators based on renewable energy sources where BSSs are used for both EV charging and energy management purposes. However, to the best of our knowledge there has been little effort on the optimal scheduling of battery charging inside a BSS, the focus of the present paper.

While there has been much work on charging schedules for generic EVs, the scheduling problem for EBs has an important difference. Unlike passenger cars that typically spend most of their time parking or taxis whose driving patterns are hard to predict, a bus usually has a tight driving schedule and follows a fixed route. Battery charging in a BSS must be scheduled so that every EB that arrives will find a battery ready for switching. While this seems very stringent, the relatively deterministic routine of EBs also means that when an EB needs its battery switched can be well predicted in advance, perhaps from historical data. In this paper we propose a model that exploits this feature and an efficient algorithm to compute an optimal charging schedule for a large BSS.

As we will see below, our goal is to schedule the battery charging in a BSS in a way that minimizes energy cost and battery degradation, taking into account real-time electricity prices, the state of charge (SOC) of returned batteries from EB arrivals, the exact times of EB arrivals and the maximum power the BSS can draw from the grid at any time. In practice these parameters may vary over time with uncertainty. A common strategy to deal with the uncertainty is to apply a receding-horizon framework, which contains two parts. First, assume all future parameters

are known (e.g., forecasts from historical data) and solve a deterministic scheduling problem. Second, update the parameters (forecasts) in real time as more information becomes available and re-solve the scheduling problem. Under this framework the deterministic scheduling problem must be solved repeatedly. Meanwhile, a finer time scale renders a better approximation of real-time systems, but also increases the scale of the scheduling problem. Therefore, an efficient algorithm is important especially for large-scale BSSs. This paper concerns the first part where we develop such an algorithm, assuming the relevant parameter values are given. Though some generic algorithms and existing solvers could also solve the scheduling problem, as we illustrate through numerical examples, the proposed algorithm is more efficient and scales much better as the size of the scheduling problem grows.

We now summarize our main contribution. The scheduling problem formulated here is a convex program with constraints that couple the charging decisions of all charging boxes in a BSS and across all times, making a direct solution inefficient. The computational efficiency of our solution is due to two features of our design. First, standard dual decomposition [17]–[21] is applied to decouple the charging decisions of different charging boxes. This decomposes the overall problem into a set of spatially decoupled local subproblems that can be solved independently, given a coordination signal. This leads to a distributed algorithm [22]–[28] that can be executed in parallel at each charging box within the BSS. Our algorithm is therefore inherently scalable as the size of the BSS grows. Second, each local subproblem solves for the optimal charging decisions of one charging box over the entire time horizon based on given (forecasted) parameter values. Instead of resorting to generic convex optimization techniques, we exploit the structure of our problem to develop a much faster direct projection method.

The remainder of this paper is organized as follows. We describe the system model and formulate our optimal scheduling problem in Section II. We develop our solution in Section III and illustrate in Section IV its computational efficiency through numerical examples. Finally, we conclude in Section V.

II. MODEL AND OPTIMAL CHARGING SCHEDULE

We first describe the scenario we study in this paper, which motivates our formal model. We then formulate the optimal scheduling problem for an EB BSS.

We generally use bold letters to denote vectors, e.g., $\boldsymbol{p}$ denotes a vector $\boldsymbol{p} \triangleq [p_c^t]_{t \in \mathbb{T}, c \in \mathbb{C}}$ and p_c^t denotes a scalar.

A. Scenario and Assumptions

We consider a single BSS and its operation over a finite horizon, e.g., five hours. An important feature of a bus service is that each bus usually has a fixed route and more or less follows a tight schedule. Its routine is relatively predictable. In particular when it will need its battery switched can be predicted in advance, perhaps from historical data. We will hence adopt a deterministic model where the sequence of EB arrivals at the BSS is known in advance.

As an EB system is often standardized, we assume that all EB batteries are identical. Typically an EB comes in for battery switching when its battery's SOC falls below a small threshold

(e.g., 20% of battery capacity). The unloaded battery is replaced with a battery that has been charged to a sufficiently high SOC (e.g., 90% of battery capacity); we refer to it as a *fully-charged battery*. The returned battery takes the place of the fully-charged battery in the charging box. Its charging process starts immediately and continues until its SOC exceeds the high threshold (becomes fully charged) and an EB arrival is assigned to this charging box for battery switching. Therefore, the total number of batteries in the BSS remains constant. We assume battery switching time is negligible compared with battery charging time.

Since the arrival times of the EBs at the BSS are deterministic, every returned battery has a similar (low) SOC and will be switched by a battery with a similar (high) SOC, we can assign *in advance* every EB to a charging box for battery switching and seek an optimal charging schedule that can *support* this pre-determined EB-to-charging-box assignment. An assignment, e.g., round-robin among the charging boxes, can be supported by a charging schedule if, under the charging schedule, every EB arrives at its assigned charging box to find a fully-charged battery.

An alternative approach is to assign an EB to a charging box only when it arrives at the BSS and the assignment depends on the SOC of all batteries in the BSS. This online assignment policy is more flexible, but greatly complicates the optimization of the charging schedule. We have adopted a pre-determined assignment both because EB routines are relatively predictable and because a pre-determined assignment creates a simple environment in which the schedule can be optimized. Under such a pre-determined assignment, each charging box knows its own EB arrival sequence in advance.

We now describe a formal model that captures the essence of this scenario.

B. BSS Model

Consider a discrete time horizon $\mathbb{T} \triangleq \{1, 2, \ldots, T\}$, and a BSS consisting of a set $\mathbb{C} \triangleq \{1, 2, \ldots, C\}$ of charging boxes. At any time slot t each charging box c contains one battery and is responsible for its charging. For each charging box $c \in \mathbb{C}$, there is a deterministic and known sequence of A_c EB arrivals, $\mathbb{A}_c \triangleq \{(t_{ca}, \pi_{ca}^r), a = 1, 2, \ldots, A_c\}$, where $t_{ca} \in \mathbb{T}$ is the arrival time of the ath EB at charging box c and π_{ca}^r is the SOC of its battery on arrival. Note that $t_{c0} = 0$ and π_{c0}^r is the SOC of the initial battery in charging box c. We will also use the notation ca to refer to the battery prepared for EB arrival a at charging box c.

Our goal is to design a charging schedule under which every EB a that arrives at its pre-assigned charging box c will find a fully-charged battery ready for switching. Immediately after time slot $t_{c(a-1)}$, $a = 1, \ldots, A_c$, i.e., the initial time 0 or the time of EB arrival $(a-1)$ at charging box c, the total time available to charge the battery ca is $t_{ca} - t_{c(a-1)}$, i.e., until EB arrival a at charging box c. Denote this interval by $\mathbb{T}_{ca} \triangleq \{t_{c(a-1)}, t_{c(a-1)} + 1, \ldots, t_{ca} - 1\}$. The basic setup is illustrated in Fig. 1.

Whether there is a feasible schedule and how to compute an optimal schedule among all feasible schedules depend on our design objective and how charging power of different charging boxes at different time slots are coupled, as we now explain.
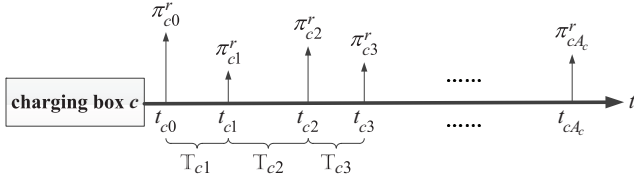
Fig. 1. Basic setup.

C. Constraints

Let p_c^t denote the charging power of charging box c at time slot t, which is the control variable. In this paper, we ignore the vehicle-to-grid (V2G) service. Then for charging box c we have

$$0 \leq p_c^t \leq p_{c,\max}, \quad t \in \mathbb{T}, c \in \mathbb{C} \tag{1}$$

where $p_{c,\max}$ is the maximum charging power of charging box c.

The total charging load of the BSS must be upper bounded:

$$\sum_{c \in \mathbb{C}} p_c^t \leq L^t, \quad t \in \mathbb{T} \tag{2}$$

where L^t is the maximum allowable load of the BSS at time slot t. This is to avoid overloading the distribution grid. We allow the limit L^t to vary over time to help realize peak shaving and valley filling.

We assume a simple linear battery SOC dynamic. For battery ca, $c \in \mathbb{C}$, $a = 1, \ldots, A_c$, its SOC evolves according to:

$$\pi_{ca}^{t+1} = \pi_{ca}^t + \gamma_c p_c^t, \quad t \in \mathbb{T}_{ca}$$

where π_{ca}^t is the SOC of battery ca at time slot t, and $\gamma_c \in (0, 1]$ denotes the charging efficiency of charging box c. Then the final SOC of that battery when it is handed over to the corresponding EB is

$$\pi_{ca}^0 + \sum_{t \in \mathbb{T}_{ca}} \gamma_c p_c^t, \quad c \in \mathbb{C}, \quad a = 1, \ldots, A_c$$

where π_{ca}^0 is the initial SOC of battery ca, and $\pi_{ca}^0 = \pi_{c(a-1)}^r$. We require that its final SOC exceed a threshold $\underline{\pi}$ and not exceed the battery capacity Π, i.e.,

$$\underline{\pi} \leq \pi_{ca}^0 + \sum_{t \in \mathbb{T}_{ca}} \gamma_c p_c^t \leq \Pi, \quad c \in \mathbb{C}, \quad a = 1, \ldots, A_c \tag{3}$$

D. Costs

The goal of the BSS is to minimize the following costs:

1) *Electricity cost.* Suppose the BSS purchases electricity from the real-time market, and let θ^t be the real-time price at time slot t. For simplicity, θ^t is assumed to be known in advance, e.g., estimated from historical data.

2) *Battery degradation.* It is well known that different charging power will cause different degrees of battery degradation. Typically, the larger the charging power is, the more severe the degradation will be. Previous studies show that battery degradation can be modeled as a quadratic function [29] or a piecewise linear function [30] of charging power. We adopt a more general model where battery degradation is a *strictly* convex and monotonically

increasing function of charging power, i.e., $D(p_c^t)$. The strict convexity of $D(\cdot)$ implies monotonically increasing marginal battery degradation, i.e., $D''(\cdot) > 0$.

3) *Low battery utilization.* Frequent battery switching causes excessive mechanical wear and tear. Thus, a battery should be charged as close to its capacity as possible before loaded onto an EB. We use the unused battery capacity as a proxy for this cost:

$$W_{ca}(\boldsymbol{p}_{ca}) \triangleq \Pi - \left(\pi_{ca}^0 + \sum_{t \in \mathbb{T}_{ca}} \gamma_c p_c^t \right) \tag{4}$$

where $\boldsymbol{p}_{ca} \triangleq [p_c^t]_{t \in \mathbb{T}_{ca}}$.

E. Optimal Charging Schedule

The scheduling problem for the BSS can be summarized as: control the charging power of all charging boxes over all time slots, so that the total cost of the BSS is minimized subject to constraints (1), (2) and (3). That is,

Primal problem

$$\min_{\boldsymbol{p}} \sum_{c \in \mathbb{C}} \left[\sum_{t \in \mathbb{T}} \left(\theta^t p_c^t + \alpha D(p_c^t) \right) + \beta \sum_{a=1}^{A_c} W_{ca}(\boldsymbol{p}_{ca}) \right]$$
$$\text{s.t. } (1)(2)(3) \tag{5}$$

where $\boldsymbol{p} \triangleq [p_c^t]_{t \in \mathbb{T}, c \in \mathbb{C}}$ and $\alpha, \beta \geq 0$ are both constant weights.

We make the following assumption:

Assumption 1: The primal problem is feasible.

An immediate implication of this assumption is that there is no duality gap between the primal problem (5) and its Lagrangian dual.

III. OUR SOLUTION

A. Dual Decomposition

The constraint (1) is completely decentralized, the constraint (2) couples the charging decisions p_c^t of all charging boxes, and the constraint (3) couples the charging decisions across time. Our algorithm decouples the charging decisions of different charging boxes, so that (5) can be solved by multiple charging boxes in parallel, greatly improving the scalability of the solution. Our solution strategy is as follows. First we define the (partial) dual problem where the constraint (2) is relaxed. We then apply the standard first-order primal-dual algorithm to solve the primal problem (5) and its dual concurrently. As we will see below, the primal iterations are carried out by the charging boxes in a distributed manner where each charging box makes its own decision based on a control signal from a central agent. The dual iterations are carried out by the central agent to update the control signal that coordinates the individual decisions of the charging boxes. See Fig. 2.

Introduce the Lagrange multiplier vector $\boldsymbol{\lambda} \triangleq [\lambda^t]_{t \in \mathbb{T}}$ with $\lambda^t \geq 0$ for the constraint (2) and the Lagrangian of (5):

$$\mathcal{L}(\boldsymbol{\lambda}, \boldsymbol{p}) \triangleq \sum_{c \in \mathbb{C}} \left[\sum_{t \in \mathbb{T}} \left(\theta^t p_c^t + \alpha D(p_c^t) \right) + \beta \sum_{a=1}^{A_c} W_{ca}(\boldsymbol{p}_{ca}) \right]$$
$$+ \sum_{t \in \mathbb{T}} \left(\sum_{c \in \mathbb{C}} p_c^t - L^t \right) \lambda^t.$$
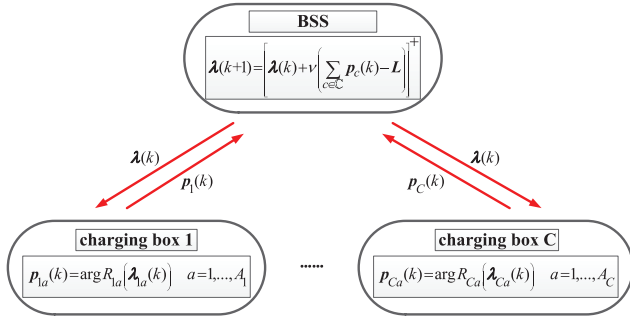
Fig. 2. Algorithm 1 for solving (5).

The dual function is:

$$F(\boldsymbol{\lambda}) = \min_{\boldsymbol{p}} \mathcal{L}(\boldsymbol{\lambda}, \boldsymbol{p}) \text{ s.t. } (1), (3)$$
$$\triangleq \sum_{c \in \mathbb{C}} S_c(\boldsymbol{\lambda}) + \Gamma(\boldsymbol{\lambda}) \tag{6}$$

where $\Gamma(\boldsymbol{\lambda}) \triangleq \sum_{c \in \mathbb{C}} \sum_{a=1}^{A_c} \beta(\Pi - \pi_{ca}^0) - \sum_{t \in \mathbb{T}} L^t \lambda^t$ and

$$S_c(\boldsymbol{\lambda}) \triangleq \min_{\boldsymbol{p}_c : (1),(3)} \sum_{t \in \mathbb{T}} \left[(\theta^t - \beta \gamma_c + \lambda^t) p_c^t + \alpha D\left(p_c^t\right) \right]$$

where the notation on the right-hand side means minimization over $\boldsymbol{p}_c \triangleq [p_c^t]_{t \in \mathbb{T}}$ subject to (1) and (3). Given $\boldsymbol{\lambda}$, the subproblem $S_c(\boldsymbol{\lambda})$ can be solved by each charging box c independently. Moreover, $S_c(\boldsymbol{\lambda})$ can be further decomposed into subproblems, each for a single battery:

$$S_c(\boldsymbol{\lambda}) = \min_{\boldsymbol{p}_c : (1),(3)} \sum_{a=1}^{A_c} \sum_{t \in \mathbb{T}_{ca}} \left[(\theta^t - \beta \gamma_c + \lambda^t) p_c^t + \alpha D\left(p_c^t\right) \right]$$
$$\triangleq \sum_{a=1}^{A_c} R_{ca}(\boldsymbol{\lambda}_{ca})$$

Note that the subproblems $R_{ca}(\boldsymbol{\lambda}_{ca})$ schedule the battery charging for EB arrivals a at charging boxes c during the intervals $\mathbb{T}_{ca}$:

Scheduling subproblem

$$R_{ca}(\boldsymbol{\lambda}_{ca}) \triangleq \min_{\boldsymbol{p}_{ca}} \sum_{t \in \mathbb{T}_{ca}} \left[(\theta^t - \beta \gamma_c + \lambda^t) p_c^t + \alpha D\left(p_c^t\right) \right]$$

$$\text{s.t. } \pi \leq \pi_{ca}^0 + \sum_{t \in \mathbb{T}_{ca}} \gamma_c p_c^t \leq \Pi \tag{7a}$$

$$0 \leq p_c^t \leq p_{c,\max}, \quad t \in \mathbb{T}_{ca} \tag{7b}$$

where $\boldsymbol{p}_{ca} \triangleq [p_c^t]_{t \in \mathbb{T}_{ca}}$ and $\boldsymbol{\lambda}_{ca} \triangleq [\lambda^t]_{t \in \mathbb{T}_{ca}}$. The dual problem is to maximize the dual function (6) over the Lagrange multiplier $\boldsymbol{\lambda}$:

Dual problem

$$\max_{\boldsymbol{\lambda}} F(\boldsymbol{\lambda})$$
$$\text{s.t. } \lambda^t \geq 0, \quad t \in \mathbb{T} \tag{8}$$

Since there is no duality gap, solving (5) is equivalent to solving (8). Given a dual optimal solution $\boldsymbol{\lambda}^*$, we can obtain a primal optimal solution $\boldsymbol{p}^*$ by solving local subproblems (7).

We propose to solve (8) by the standard gradient projection algorithm:

$$\boldsymbol{\lambda}(k+1) = \left[\boldsymbol{\lambda}(k) + \nu \frac{\partial F}{\partial \boldsymbol{\lambda}}(\boldsymbol{\lambda}(k)) \right]^+$$
$$= \left[\boldsymbol{\lambda}(k) + \nu \left(\sum_{c \in \mathbb{C}} \boldsymbol{p}_c(k) - \boldsymbol{L} \right) \right]^+ \tag{9}$$

where $\boldsymbol{L} \triangleq [L^t]_{t \in \mathbb{T}}$, $[x]^+ = \max\{x, 0\}$, and $k \in \mathbb{N}^+$ represents the iteration index. As long as the step size $\nu > 0$ is sufficiently small, the gradient algorithm will approach a limit point that is optimal [31].

Specifically our algorithm to solve the optimal scheduling problem (5) is a standard gradient projection algorithm to solve its Lagrangian dual (8). It can be carried out iteratively by the BSS and individual charging boxes. In each iteration k, given the Lagrange multiplier vector $\boldsymbol{\lambda}(k)$, each charging box c solves its own scheduling subproblems (7) for the entire time horizon $\mathbb{T}_{ca}, a = 1, \ldots, A_c$, to determine charging power $\boldsymbol{p}_c(k)$ for the next iteration. The BSS updates $\boldsymbol{\lambda}(k)$ to $\boldsymbol{\lambda}(k+1)$ according to (9) to coordinate the charging boxes in the next iteration. The iterations between the BSS and charging boxes continue until $(\boldsymbol{p}(k), \boldsymbol{\lambda}(k))$ converges (approximately) to the global optimal $(\boldsymbol{p}^*, \boldsymbol{\lambda}^*)$. This is summarized in Algorithm 1 and illustrated in Fig. 2.

B. Direct Projection Method: Basic Idea

In Algorithm 1, the update on the dual variables $\boldsymbol{\lambda}(k)$ is straightforward but centralized. The update on the primal variables $\boldsymbol{p}_{ca}(k)$ requires solving (7) at every charging box $c \in \mathbb{C}$ for each EB arrival $a = 1, \ldots, A_c$. Clearly (7) has a solution since its feasible set is nonempty and compact. Since (7) is convex with only temporally coupled constraints, it can in principle be solved using standard convex optimization techniques. In this section we derive an alternative method to compute $\boldsymbol{p}_{ca}(k)$ directly instead of iteratively. Compared with generic algorithms such as the interior point method, active set method and sequential quadratic programming (SQP) method, and existing solvers such as MOSEK and SeDuMi, our algorithm is more efficient and scalable (see case studies below), making it more suitable for real-time solution of large BSSs, especially when their parameters are time-varying.

In this subsection we drop the iteration index k to simplify notation.

Since (7) is convex, the Karush-Kuhn-Tucker (KKT) condition is necessary and sufficient for optimality. Let

τ_{ca}, σ_{ca} be the Lagrange multipliers corresponding to the upper and lower bounds in (7a), respectively, and $\boldsymbol{\xi}_{ca} \triangleq [\xi_c^t]_{t\in\mathbb{T}_{ca}}, \boldsymbol{\eta}_{ca} \triangleq [\eta_c^t]_{t\in\mathbb{T}_{ca}}$ be those in (7b), respectively. Then the KKT condition is:

Primal feasibility

$$(\tau_{ca}) \ \pi_{ca}^0 + \sum_{t\in\mathbb{T}_{ca}} \gamma_c p_c^t - \Pi \leq 0 \tag{10a}$$

$$(\sigma_{ca}) \ \pi - \pi_{ca}^s - \sum_{t\in\mathbb{T}_{ca}} \gamma_c p_c^t \leq 0 \tag{10b}$$

$$(\xi_c^t) \ p_c^t - p_{c,\max} \leq 0, \ t \in \mathbb{T}_{ca} \tag{10c}$$

$$(\eta_c^t) \ 0 - p_c^t \leq 0, \ t \in \mathbb{T}_{ca} \tag{10d}$$

Stationarity

$$\theta^t - \beta\gamma_c + \lambda^t + \alpha D'\left(p_c^t\right) + \gamma_c\tau_{ca} - \gamma_c\sigma_{ca} + \xi_c^t - \eta_c^t = 0,$$
$$t \in \mathbb{T}_{ca} \tag{11}$$

Dual feasibility

$$\tau_{ca}, \ \sigma_{ca} \geq 0 \tag{12a}$$

$$\xi_c^t, \ \eta_c^t \geq 0, \ t \in \mathbb{T}_{ca} \tag{12b}$$

Complementary slackness

$$\tau_{ca}\left(\pi_{ca}^0 + \sum_{t\in\mathbb{T}_{ca}} \gamma_c p_c^t - \Pi\right) = 0 \tag{13a}$$

$$\sigma_{ca}\left(\pi - \pi_{ca}^0 - \sum_{t\in\mathbb{T}_{ca}} \gamma_c p_c^t\right) = 0 \tag{13b}$$

$$\xi_c^t\left(p_c^t - p_{c,\max}\right) = 0, \ t \in \mathbb{T}_{ca} \tag{13c}$$

$$\eta_c^t\left(0 - p_c^t\right) = 0, \ t \in \mathbb{T}_{ca} \tag{13d}$$

For each $t \in \mathbb{T}_{ca}$ define the following functions of scalars τ_{ca} and σ_{ca}:

$$p_c^t(\tau_{ca}, \sigma_{ca}) = \left[(D')^{-1}\left(\frac{\gamma_c(\sigma_{ca} - \tau_{ca} + \beta) - \theta^t - \lambda^t}{\alpha}\right)\right]_0^{p_{c,\max}} \tag{14a}$$

$$\xi_c^t(\tau_{ca}, \sigma_{ca}) = \left[\gamma_c(\sigma_{ca} - \tau_{ca} + \beta) - \theta^t - \lambda^t - \alpha D'(p_{c,\max})\right]_0 \tag{14b}$$

$$\eta_c^t(\tau_{ca}, \sigma_{ca}) = \left[-\gamma_c(\sigma_{ca} - \tau_{ca} + \beta) + \theta^t + \lambda^t + \alpha D'(0)\right]_0 \tag{14c}$$

where $[x]_0^y = \max\{\min\{x, y\}, 0\}$ and $[x]_0 = \max\{x, 0\}$. The following theorem expresses the primal variables $\boldsymbol{p}_{ca}$ and the dual variables $(\boldsymbol{\xi}_{ca}, \boldsymbol{\eta}_{ca})$ in terms of (τ_{ca}, σ_{ca}). It is proved in Appendix A.

Theorem 1: Any scalars $(\tau_{ca}, \sigma_{ca}) \geq 0$ together with $p_c^t(\tau_{ca}, \sigma_{ca}), \xi_c^t(\tau_{ca}, \sigma_{ca})$ and $\eta_c^t(\tau_{ca}, \sigma_{ca})$ given by (14) satisfy (10c), (10d), (11), (12), (13c) and (13d).

Theorem 1 implies that, to solve the subproblem (7), it is sufficient to search for a Lagrange multiplier pair $(\tau_{ca}^*, \sigma_{ca}^*) \geq 0$ such that $(\tau_{ca}^*, \sigma_{ca}^*)$ together with $p_c^t(\tau_{ca}^*, \sigma_{ca}^*), \xi_c^h(\tau_{ca}^*, \sigma_{ca}^*)$ and $\eta_c^t(\tau_{ca}^*, \sigma_{ca}^*)$ given by (14) *also* satisfy (10a), (10b), (13a), (13b).

Assumption 2: $\pi < \Pi$.
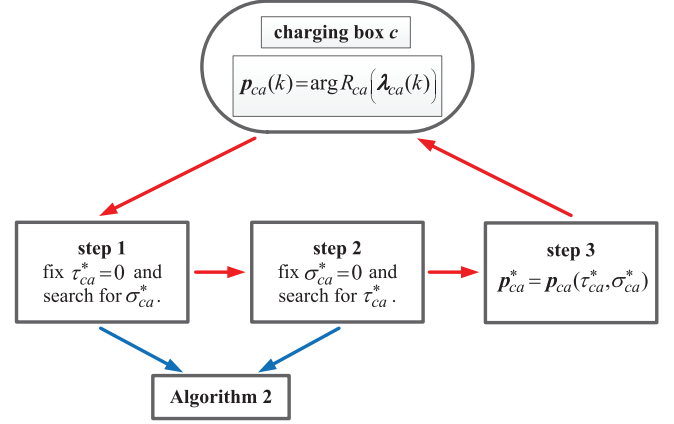
Fig. 3. Direct projection method for solving (7).

This assumption implies that at least one of τ_{ca}^* and σ_{ca}^* is zero at optimality. This is because, under complementary slackness, $\tau_{ca}^* > 0$ implies $\pi_{ca}^0 + \sum_{t\in\mathbb{T}_{ca}} \gamma_c p_c^{t*} = \Pi$ and $\sigma_{ca}^* > 0$ implies $\pi_{ca}^0 + \sum_{t\in\mathbb{T}_{ca}} \gamma_c p_c^{t*} = \pi$. Therefore, it is impossible to have both $\tau_{ca}^* > 0$ and $\sigma_{ca}^* > 0$ at optimality.

This motivates the following strategy for solving the scheduling subproblem (7) for each charging box $c \in \mathbb{C}$ and each EB arrival $a = 1, \ldots, A_c$:

Step 1: Fix $\tau_{ca}^* = 0$. This enforces (13a). Search for σ_{ca}^* such that (14) satisfies (10a), (10b) and (13b).

If such a σ_{ca}^* does not exist, go to Step 2. Otherwise, the optimal Lagrange multiplier pair is $(0, \sigma_{ca}^*)$; go to Step 3.

Step 2: Fix $\sigma_{ca}^* = 0$. This enforces (13b). Search for τ_{ca}^* such that (14) satisfies (10a), (10b) and (13a).

If successful, the optimal Lagrange multiplier pair is $(\tau_{ca}^*, 0)$; go to Step 3.

Step 3: Apply (14) to compute the optimal charging power $p_c^{t*} = p_c^t(\tau_{ca}^*, \sigma_{ca}^*)$ for $t \in \mathbb{T}_{ca}$.

This strategy is illustrated in Fig. 3. We now describe the search algorithm for Step 1. The search algorithm for Step 2 is similar.

C. Direct Projection Method: Algorithm for Step 1

Fix $\tau_{ca}^* = 0$ and define for scalar $\sigma_{ca} \geq 0$

$$h_{ca}(\sigma_{ca}) \triangleq \sum_{t\in\mathbb{T}_{ca}} \gamma_c \, p_c^t(0, \sigma_{ca})$$

From (14) $p_c^t(0, \sigma_{ca})$ can be expressed as follows:

$$p_c^t(0, \sigma_{ca}) = \begin{cases} 0, & \sigma_{ca} \leq \frac{\alpha D'(0) + \theta^t + \lambda^t - \beta\gamma_c}{\gamma_c} \\ (D')^{-1}\left(\frac{\gamma_c(\sigma + \beta) - \theta^t - \lambda^t}{\alpha}\right), & \text{otherwise} \\ p_{c,\max}, & \sigma_{ca} \geq \frac{\alpha D'(p_{c,\max}) + \theta^t + \lambda^t - \beta\gamma_c}{\gamma_c} \end{cases}$$

Note that the function $p_c^t(0, \sigma_{ca})$ is piecewise and monotonically increasing in σ_{ca}, and so is $h_{ca}(\sigma_{ca})$. With the definition of $h_{ca}(\sigma_{ca})$, the task is turned into searching for a $\sigma_{ca} \geq 0$ that satisfies

$$\begin{cases} \pi - \pi_{ca}^0 \leq h_{ca}(\sigma_{ca}) \leq \Pi - \pi_{ca}^0 & \text{(15a)} \\ \sigma_{ca}\left[\pi - \pi_{ca}^0 - h_{ca}(\sigma_{ca})\right] = 0 & \text{(15b)} \end{cases}$$

There are three possible cases:

- *Case 1: solution σ_{ca}^* does not exist*. This is the case if either $\sum_{t \in \mathbb{T}_{ca}} \gamma_c \, p_{c,\max} < \pi - \pi_{ca}^0$ or $h_{ca}(0) > \Pi - \pi_{ca}^0$ in which the condition (15a) cannot be satisfied. In this case, go to Step 2.
- *Case 2: (15) is satisfied for $\sigma_{ca}^* = 0$*. This is the case if $\pi - \pi_{ca}^0 \le h_{ca}(0) \le \Pi - \pi_{ca}^0$. Then the optimal Lagrange multiplier pair is $(\tau_{ca}^*, \sigma_{ca}^*) = (0, 0)$; go to Step 3.
- *Case 3: (15) is satisfied for $\sigma_{ca}^* > 0$*. This is the case if $h_{ca}(0) < \pi - \pi_{ca}^0 \le h_{ca}(\sigma_{ca}^*) \le \Pi - \pi_{ca}^0$. Then the optimal Lagrange multiplier pair is $(0, \sigma_{ca}^*)$; go to Step 3.

The key is therefore to solve for an $\sigma_{ca}^* > 0$ in Case 3 that satisfies

$$h_{ca}(\sigma_{ca}) = \pi - \pi_{ca}^0. \qquad (16)$$

We can solve (16) efficiently for an $\sigma_{ca}^* > 0$ by utilizing the piecewise and monotonic property of $h_{ca}(\sigma_{ca})$. Note that $h_{ca}(\sigma_{ca})$ is the summation of a number $t_{c(a+1)} - t_{ca}$ of $p_c^t(0, \sigma_{ca}), t \in \mathbb{T}_{ca}$, and each $p_c^t(0, \sigma_{ca})$ has two breakpoints. Thus, $h_{ca}(\sigma_{ca})$ has $2(t_{c(a+1)} - t_{ca})$ breakpoints in total, i.e., $(\alpha D'(0) + \theta^t + \lambda^t - \beta \gamma_c)/\gamma_c$ and $(\alpha D'(p_{c,\max}) + \theta^t + \lambda^t - \beta \gamma_c)/\gamma_c$ for $t \in \mathbb{T}_{ca}$. Let $\sigma_{ca}^1, \sigma_{ca}^2, \ldots, \sigma_{ca}^N$ denote all the positive and non-repeated breakpoints among the $2(t_{c(a+1)} - t_{ca})$ breakpoints, where $N \le 2(t_{c(a+1)} - t_{ca})$. Then, arrange them in ascending order, i.e., $0 =: \sigma_{ca}^0 < \sigma_{ca}^1 < \sigma_{ca}^2 < \cdots < \sigma_{ca}^N$. If $\sigma_{ca}^* = \sigma_{ca}^0$ then $h_{ca}(\sigma_{ca}^*) = h_{ca}(0)$, and if $\sigma_{ca}^* \ge \sigma_{ca}^N$ then $h_{ca}(\sigma_{ca}^*) = \sum_{t \in \mathbb{T}_{ca}} \gamma_c \, p_{c,\max}$. Hence we can use binary search to quickly locate σ_{ca}^* between two breakpoints, as detailed from Line 7 to 18 in Algorithm 2.

The above procedure narrows the range for σ_{ca}^* to the interval $[\sigma_{ca}^l, \sigma_{ca}^r]$. Within this interval, we can readily obtain σ_{ca}^* using the Newton-Raphson method. Once the Lagrange multiplier pair $(0, \sigma_{ca}^*)$ is obtained, the optimal solution $[p_c^{t*}]_{t \in \mathbb{T}_{ca}}$ to the subproblem (7) can be evaluated using (14).

IV. NUMERICAL RESULTS

We first study a small BSS with 5 charging boxes in detail and then scale up the number of charging boxes to 400 to illustrate scalability.

There are 5 batteries with initial SOCs in a decreasing order: 0.7, 0.68, 0.66, 0.64 and 0.62. We consider a time horizon with 17 time slots. The arrival process of EBs is shown in Fig. 4, which gives the number of EBs arrivals in each time slot. The expected initial SOC of every returned battery is randomly given around 0.2. The real-time prices θ^t, shown in Fig. 5(a), are taken from the RTP program in Singapore from 6 a.m. to 11 p.m. on September 18, 2014. The maximum allowable loads L^t are given accordingly in Fig. 5(b). We use a quadratic function for battery degradation: $D(p_c^t) = 0.5 p_c^{t\,2}$. The battery capacity is set at 139.68 kWh (388 V, 360 Ah) for all batteries. Other parameters are listed in Table I. All simulation results are obtained by MATLAB R2012a running on a laptop PC with Intel Core i7-3632QM CPU@2.20 GHz, 8 GB RAM, and 64-bit Windows 8.1 OS.

Algorithm 2: Step 1 of direct projection method

---

1   fix $\tau_{ca}^* = 0$;
2   **if** $h_{ca}(0) > \Pi - \pi_{ca}^0$ or $\sum_{t \in \mathbb{T}_{ca}} \gamma_c p_{c,\max} < \pi - \pi_{ca}^0$ **then**
3   **return** σ_{ca}^* does not exist when $\tau_{ca}^* = 0$ (go to Step 2);
4   **else if** $h_{ca}(0) \ge \pi - \pi_{ca}^0$ **then**
5   **return** $\sigma_{ca}^* = 0$;
6   **else**
7     $l \leftarrow 0, \ r \leftarrow N$;
8   **while** $r - l > 1$ **do**
9       $n \leftarrow \lfloor \frac{1}{2}(l + r) \rfloor$, where $\lfloor \cdot \rfloor$ is the floor function;
10      $R \leftarrow h_{ca}(\sigma_{ca}^n)$;
11   **if** $R = \pi - \pi_{ca}^0$ **then**
12   **return** $\sigma_{ca}^* = \sigma_{ca}^n$;
13   **else if** $R < \pi - \pi_{ca}^0$ **then**
14       $l \leftarrow n$;
15   **else**
16       $r \leftarrow n$;
17   **end if**
18   **end while**
19   **return** $\sigma_{ca}^* = h_{ca}^{-1}(\pi - \pi_{ca}^0), \quad \sigma_{ca}^* \in [\sigma_{ca}^l, \sigma_{ca}^r]$
20 **end if**
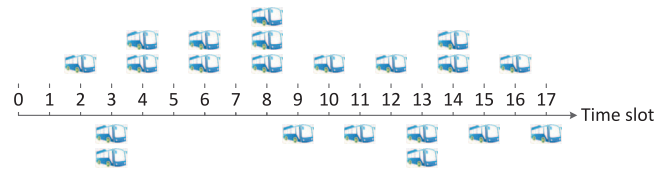
Fig. 4. Arrival process of EBs.

The proposed approach converges quickly. This is illustrated in Fig. 6(a) and (b) for the dual variable $\lambda^t(k)$ and primal variables $p_c^t(k)$ at time slot $t = 8$. The resulting optimal charging schedule is shown in Fig. 7. When possible, all charging boxes tend to charge their batteries at low electricity prices. Their schedules are coordinated through the Lagrange multiplier $\boldsymbol{\lambda}$ so that those boxes with more stringent deadlines will charge with a higher priority. On the whole, the load profile of each charging box evolves moderately with an opposite trend of real-time prices. Fig. 8 shows the SOC dynamics, where a sudden fall indicates the occurrence of battery switching. All available time of each charging interval is fully utilized. The proposed approach achieves the optimal cost of 506.9 SGD.

For comparison, Fig. 9 shows a greedy charging process where the batteries are charged as fast as possible until the full SOC π, with higher charging power for batteries with more stringent deadlines. Unlike the proposed approach, this greedy algorithm results in an intermittent load profile for each charging box, which means some batteries need to wait for charging until others finish. It will weaken the BSS's ability to deal with emergency, e.g., unexpected massive EB arrivals. The corresponding SOC dynamics are shown in Fig. 10, which reveals that the greedy algorithm neither makes full use of low-price periods nor penalizes low battery utilization. The total cost is 576.1 SGD by the greedy algorithm. Thus through comparison the proposed approach saves 12% in cost while fulfilling all battery switching requests of EBs.
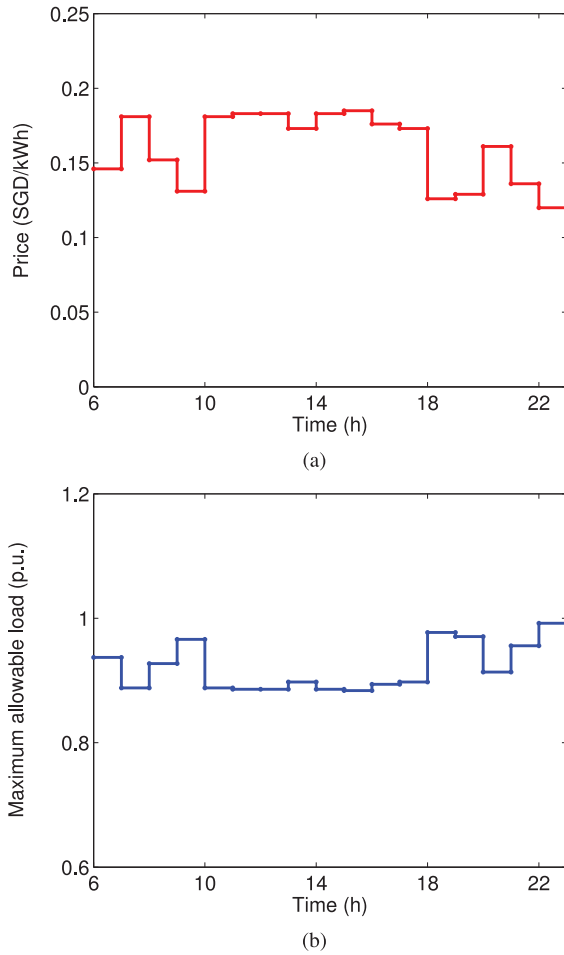
Fig. 5. (a) Real-time prices θ^t. (b) Maximum allowable loads L^t.

TABLE I
PARAMETER SETUP

Parameter	Π	π	$p_{\max}$	γ	α	β
Value	1	0.9	0.3	0.24	1	1

We then study the scalability of the proposed approach when we increase the number of the charging boxes in the BSS to 400. Meanwhile, we consider a finer time scale, e.g., a 5-hour time window with 5 minutes for each time slot, so the time horizon covers 60 time slots. Other parameters are scaled up accordingly, but the number of EBs assigned to each charging box remains unchanged. As shown in Fig. 11(a), as the number of the charging boxes rises, the number of iteration the proposed approach takes to converge increases almost linearly. The average time for each iteration varies little because the total number of EBs assigned to each charging box is unchanged, as shown in Fig. 11(b).

Fig. 12 compares the proposed approach with the interior point method, active set method and SQP method in terms of the total computation time, given the same accuracy requirement. The three generic algorithms, realized by their standard MATLAB solvers, are also combined with dual decomposition to enable distributed computation, which we refer to as three distributed algorithms. As seen in Fig. 12, the proposed approach
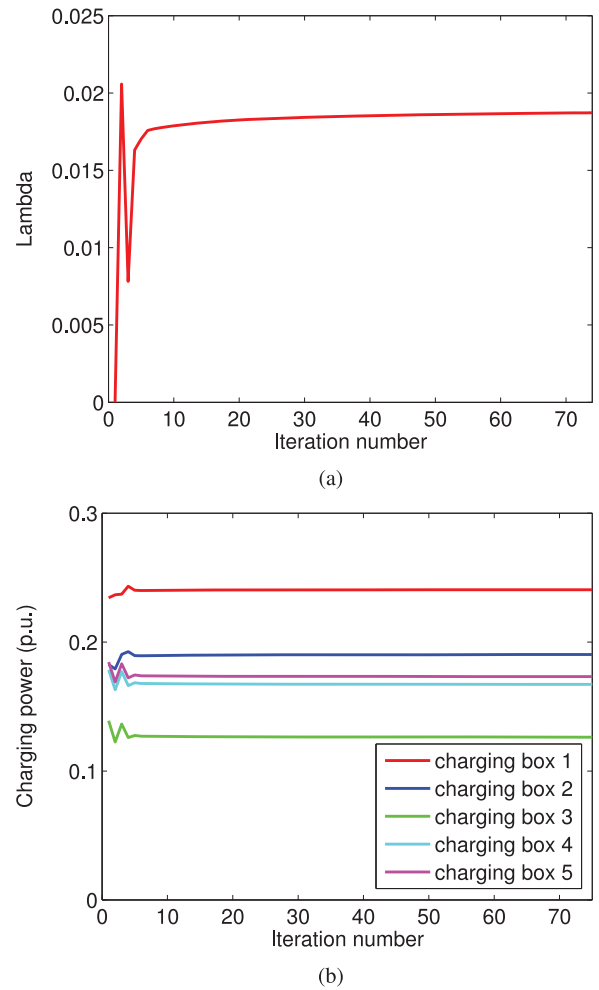
Fig. 6. Variables (a) $\lambda^8(k)$ and (b) charging power $p_c^8(k)$ for time slot 8 converge quickly in the iteration number k.
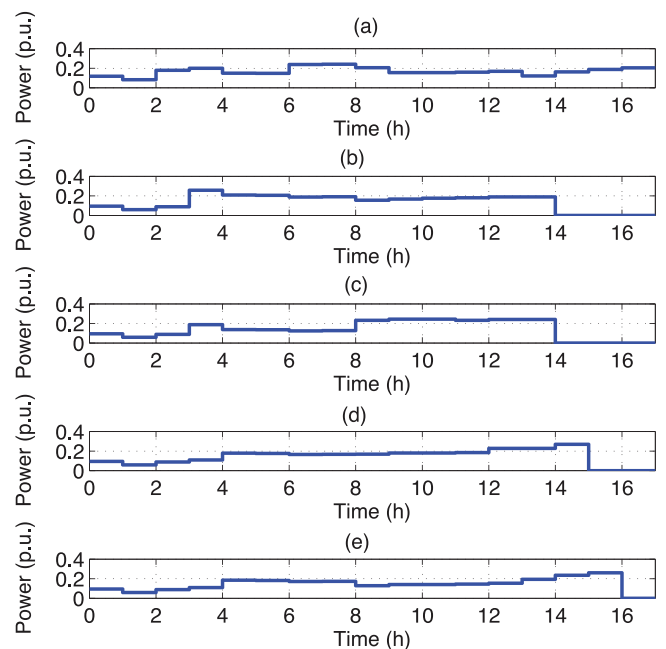
Fig. 7. Optimal battery charging process p_c^{t*}. (a) Scheduled charging box 1. (b) Scheduled charging box 2. (c) Scheduled charging box 3. (d) Scheduled charging box 4. (e) Scheduled charging box 5.
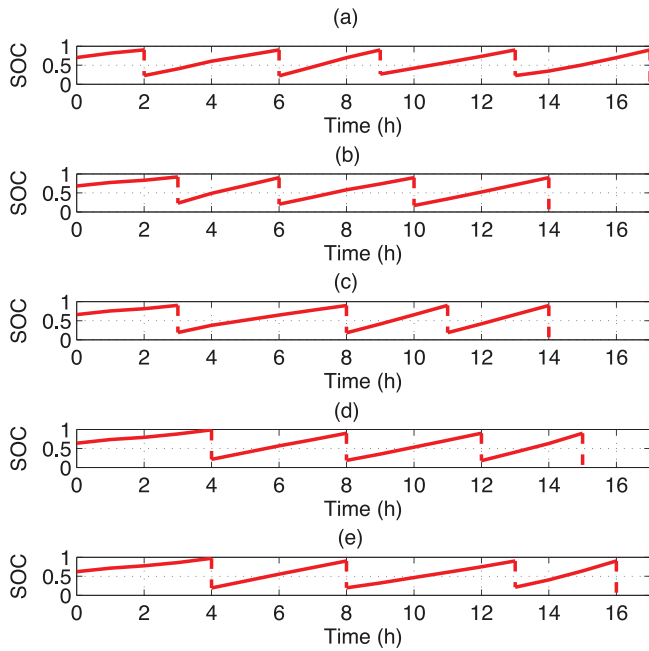
Fig. 8. Optimal battery SOC dynamics π_c^{t*}. (a) SOC dynamics of batteries in charging box 1. (b) SOC dynamics of batteries in charging box 2. (c) SOC dynamics of batteries in charging box 3. (d) SOC dynamics of batteries in charging box 4. (e) SOC dynamics of batteries in charging box 5.
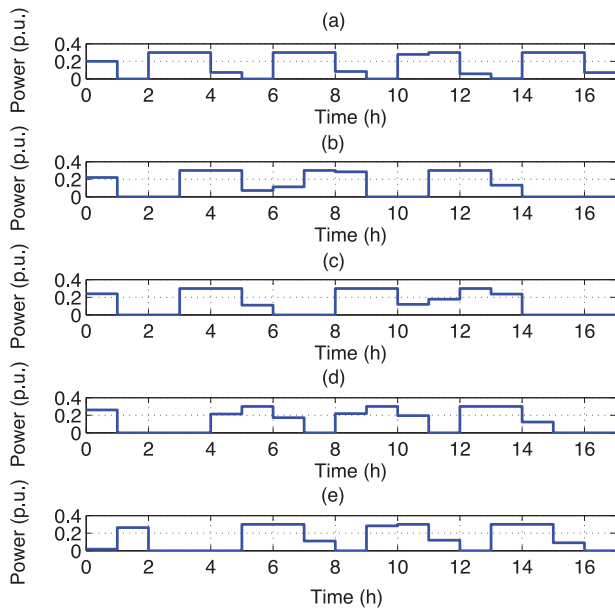
Fig. 9. Greedy battery charging process p_c^t. (a) Unscheduled charging box 1. (b) Unscheduled charging box 2. (c) Unscheduled charging box 3. (d) Unscheduled charging box 4. (e) Unscheduled charging box 5.

is far more efficient, which shows the computational advantage of the direct projection method.

Besides, to show the advantage of distributed and parallel computation, the proposed approach is also compared with some centralized algorithms/solvers including the interior point method[1], CVX-supported MOSEK and SeDuMi, which means

[1]The active set method and SQP method fail to solve the primal problem (5) in a centralized manner within a minute, even for a BSS size of 40 charging boxes.
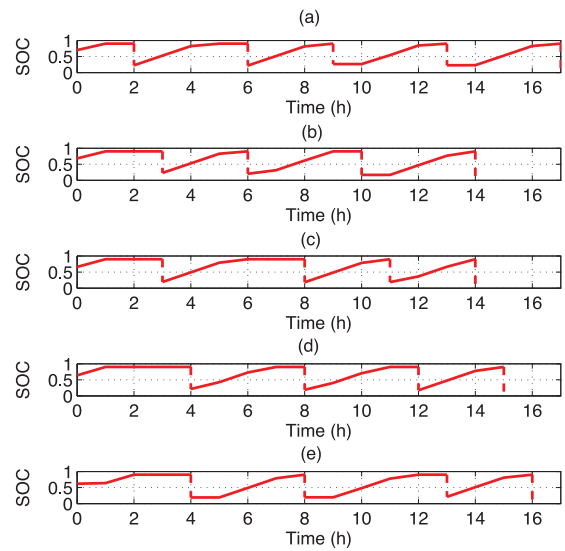
Fig. 10. Greedy battery SOC dynamics π_c^t. (a) SOC dynamics of batteries in charging box 1. (b) SOC dynamics of batteries in charging box 2. (c) SOC dynamics of batteries in charging box 3. (d) SOC dynamics of batteries in charging box 4. (e) SOC dynamics of batteries in charging box 5.
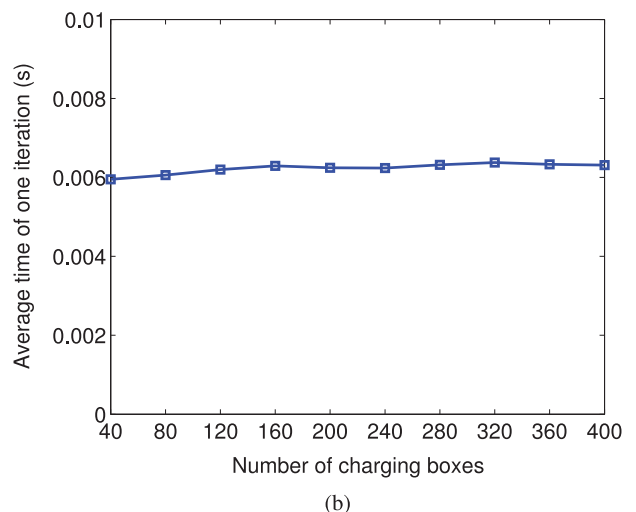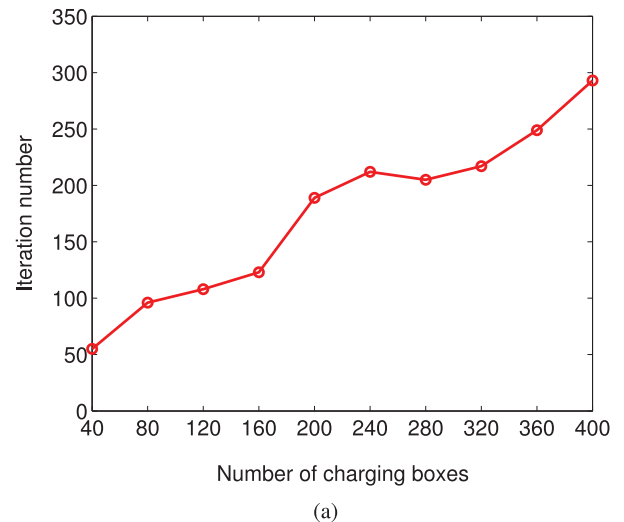
Fig. 11. Scalability.
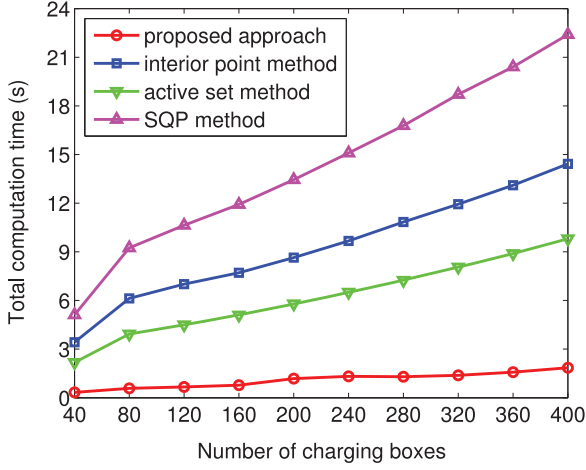
Fig. 12. Comparison with distributed algorithms.
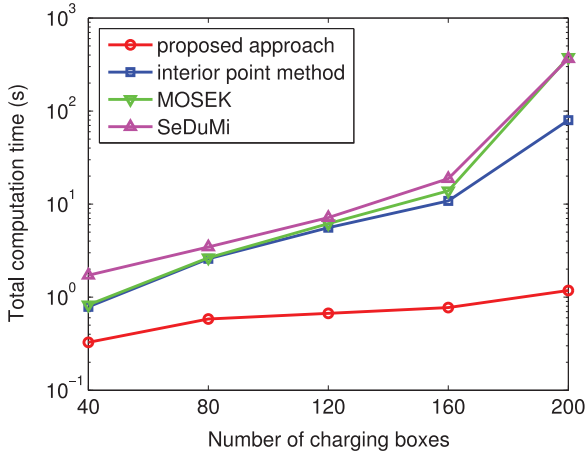
Fig. 13. Comparison with centralized algorithms/solvers.

directly applying the corresponding approach to the primal problem (5). In terms of MOSEK and SeDuMi, CVXGEN is first applied to generate clean, fast and fully-custom code, and then MOSEK and SeDuMi are selected as the default CVX solver to address the primal problem (5). The comparison result is illustrated in Fig. 13, showing that the proposed approach, which is distributedly computed, is much more efficient and performs better in scalability.

V. CONCLUSION

In this paper, the optimal schedule of battery charging in a BSS for EBs is investigated, which aims to fulfill the battery switching requests of EBs and minimize the total cost of the BSS. Every EB arrival is assigned to a specific charging box and we schedule battery charging in the BSS so that every EB arrives to find a battery ready for switching. The scheduling problem is formulated as a convex program with both spatially and temporally coupled constraints. To tackle spatially coupled constraints, dual decomposition is introduced, which decomposes the original problem into a series of local subproblems to be solved separately. In allusion to each subproblem, a direct projection method is designed. Using the proposed approach, the

scheduling problem can be addressed efficiently in a distributed manner.

APPENDIX A
PROOF OF THEOREM 1

Since (14) obviously satisfies (10c), (10d) and (12), we shall mainly focus on the proofs for (11), (13c) and (13d). It is important to notice that *when $D'(\cdot)$ is monotonically non-decreasing, so is $(D')^{-1}(\cdot)$.*

For (11), we consider the following 3 cases.
Case 1:

$$(D')^{-1}\left(\frac{\gamma_c(\sigma_{ca} - \tau_{ca} + \beta) - \theta^t - \lambda^t}{\alpha}\right) > p_{c,\max}$$

$$\Rightarrow \begin{cases} p_c^t = p_{c,\max} \\ \gamma_c(\sigma_{ca} - \tau_{ca} + \beta) - \theta^t - \lambda^t - \alpha D'(p_{c,\max}) > 0 \\ -\gamma_c(\sigma_{ca} - \tau_{ca} + \beta) + \theta^t + \lambda^t + \alpha D'(0) < 0 \end{cases}$$

$$\Rightarrow \begin{cases} \xi_c^t = \gamma_c(\sigma_{ca} - \tau_{ca} + \beta) - \theta^t - \lambda^t - \alpha D'(p_{c,\max}) \\ \eta_c^t = 0 \end{cases}$$

Hence,

$$\theta^t - \beta\gamma_c + \lambda^t + \alpha D'\left(p_c^t\right) + \gamma_c\tau_{ca} - \gamma_c\sigma_{ca} + \xi_c^t - \eta_c^t$$
$$= \theta^t - \beta\gamma_c + \lambda^t + \alpha D'(p_{c,\max}) + \gamma_c\tau_{ca} - \gamma_c\sigma_{ca}$$
$$\quad + \gamma_c(\sigma_{ca} - \tau_{ca} + \beta) - \theta^t - \lambda^t - \alpha D'(p_{c,\max}) - 0$$
$$= 0$$

Case 2:

$$0 \le (D')^{-1}\left(\frac{\gamma_c(\sigma_{ca} - \tau_{ca} + \beta) - \theta^t - \lambda^t}{\alpha}\right) \le p_{c,\max}$$

$$\Rightarrow \begin{cases} p_c^t = (D')^{-1}\left(\frac{\gamma_c(\sigma_{ca} - \tau_{ca} + \beta) - \theta^t - \lambda^t}{\alpha}\right) \\ \gamma_c(\sigma_{ca} - \tau_{ca} + \beta) - \theta^t - \lambda^t - \alpha D'(p_{c,\max}) \le 0 \\ -\gamma_c(\sigma_{ca} - \tau_{ca} + \beta) + \theta^t + \lambda^t + \alpha D'(0) \le 0 \end{cases}$$

$$\Rightarrow \begin{cases} D'\left(p_c^t\right) = \frac{\gamma_c(\sigma_{ca} - \tau_{ca} + \beta) - \theta^t - \lambda^t}{\alpha} \\ \xi_c^t = 0 \\ \eta_c^t = 0 \end{cases}$$

Hence,

$$\theta^t - \beta\gamma_c + \lambda^t + \alpha D'\left(p_c^t\right) + \gamma_c\tau_{ca} - \gamma_c\sigma_{ca} + \xi_c^t - \eta_c^t$$
$$= \theta^t - \beta\gamma_c + \lambda^t + \alpha\frac{\gamma_c(\sigma_{ca} - \tau_{ca} + \beta) - \theta^t - \lambda^t}{\alpha}$$
$$\quad + \gamma_c\tau_{ca} - \gamma_c\sigma_{ca} + 0 - 0$$
$$= 0$$

Case 3:

$$(D')^{-1}\left(\frac{\gamma_c(\sigma_{ca} - \tau_{ca} + \beta) - \theta^t - \lambda^t}{\alpha}\right) < 0$$

$$\Rightarrow \begin{cases} p_c^t = 0 \\ \gamma_c(\sigma_{ca} - \tau_{ca} + \beta) - \theta^t - \lambda^t - \alpha D'(p_{c,\max}) < 0 \\ -\gamma_c(\sigma_{ca} - \tau_{ca} + \beta) + \theta^t + \lambda^t + \alpha D'(0) > 0 \end{cases}$$

$$\Rightarrow \begin{cases} \xi_c^t = 0 \\ \eta_c^t = -\gamma_c(\sigma_{ca} - \tau_{ca} + \beta) + \theta^t + \lambda^t + \alpha D'(0) \end{cases}$$

Hence,

$$
\begin{aligned}
&\theta^t - \beta\gamma_c + \lambda^t + \alpha D'\left(p_c^t\right) + \gamma_c\tau_{ca} - \gamma_c\sigma_{ca} + \xi_c^t - \eta_c^t \\
&= \theta^t - \beta\gamma_c + \lambda^t + \alpha D'(0) + \gamma_c\tau_{ca} - \gamma_c\sigma_{ca} + 0 \\
&\quad - \left[-\gamma_c(\sigma_{ca} - \tau_{ca} + \beta) + \theta^t + \lambda^t + \alpha D'(0) \right] \\
&= 0
\end{aligned}
$$

For (13c), we consider the following 2 cases.
Case 1:

$$
\begin{aligned}
&\gamma_c(\sigma_{ca} - \tau_{ca} + \beta) - \theta^t - \lambda^t - \alpha D'(p_{c,\max}) < 0 \\
&\Rightarrow \xi_c^t = 0 \\
&\Rightarrow \xi_c^t\left(p_c^t - p_{c,\max}\right) = 0
\end{aligned}
$$

Case 2:

$$
\begin{aligned}
&\gamma_c(\sigma_{ca} - \tau_{ca} + \beta) - \theta^t - \lambda^t - \alpha D'(p_{c,\max}) \geq 0 \\
&\Rightarrow (D')^{-1}\left(\frac{\gamma_c(\sigma_{ca} - \tau_{ca} + \beta) - \theta^t - \lambda^t}{\alpha} \right) > p_{c,\max} \\
&\Rightarrow p_c^t = p_{c,\max} \\
&\Rightarrow \xi_c^t\left(p_c^t - p_{c,\max}\right) = 0
\end{aligned}
$$

For (13d), we consider the following 2 cases.
Case 1:

$$
\begin{aligned}
&-\gamma_c(\sigma_{ca} - \tau_{ca} + \beta) + \theta^t + \lambda^t + \alpha D'(0) < 0 \\
&\Rightarrow \eta_c^t = 0 \\
&\Rightarrow \eta_c^t\left(0 - p_c^t\right) = 0
\end{aligned}
$$

Case 2:

$$
\begin{aligned}
&-\gamma_c(\sigma_{ca} - \tau_{ca} + \beta) + \theta^t + \lambda^t + \alpha D'(0) \geq 0 \\
&\Rightarrow (D')^{-1}\left(\frac{\gamma_c(\sigma_{ca} - \tau_{ca} + \beta) - \theta^t - \lambda^t}{\alpha} \right) \leq 0 \\
&\Rightarrow p_c^t = 0 \\
&\Rightarrow \eta_c^t\left(0 - p_c^t\right) = 0
\end{aligned}
$$

This completes the proof.

REFERENCES

[1] A. Ipakchi and F. Albuyeh, "Grid of the future," *IEEE Power Energy Mag.*, vol. 7, no. 2, pp. 52–62, 2009.

[2] K. Clement-Nyns, E. Haesen, and J. Driesen, "The impact of charging plug-in hybrid electric vehicles on a residential distribution grid," *IEEE Trans. Power Syst.*, vol. 25, no. 1, pp. 371–380, Feb. 2010.

[3] G. Su, D. Xie, Y. Xue, C. Fang, Y. Zhang, and K. Li, "Information fusion for intelligent EV charging-discharging-storage integrated station," in *Intelligent Computing in Smart Grid and Electrical Vehicles.* New York, NY, USA: Springer, 2014, pp. 434–448.

[4] M. Kumar, V. Gunawat, S. Swami, D. Prajapati, B. Naik, M. Singh, and P. Kumar, "Analysis of implementing the electric city bus and its coordination with the grid," in *Proc. Annu. IEEE India Conf.*, Dec. 2012, pp. 974–978.

[5] X. Hu, N. Murgovski, L. Johannesson, and B. Egardt, "Energy efficiency analysis of a series plug-in hybrid electric bus with different energy management strategies and battery sizes," *Appl. Energy*, vol. 111, pp. 1001–1009, 2013.

[6] F. Mapelli, D. Tarsitano, D. Annese, M. Sala, and G. Bosia, "A study of urban electric bus with a fast charging energy storage system based on lithium battery and supercapacitors," in *Proc. 8th Int. Conf. Exhibition on Ecological Vehicles and Renewable Energies*, 2013, pp. 1–9.

[7] X. Wu, T. Jiang, J. Du, and C. Hu, "Comparison of different driving cycles control effects of an extended-range electric bus," in *Proc. Int. Conf. Meas., Inf. Control*, Aug. 2013, vol. 02, pp. 1073–1076.

[8] J. Chen, J. Wu, X. Wu, and J. Du, "Study on energy management strategy based on DP for range extended electric bus in Chinese driving cycles," in *Proc. IEEE Asia–Pacific Conf. Expo Transportation Electrification*, Aug. 2014, pp. 1–5.

[9] D. Wang, P. Li, Y.-Z. Bao, C.-H. Zhou, and J. Wu, "Charging optimization for electric bus based on time-of-use price," *J. Chang'an Univ. (Natural Science Ed.)*, vol. 3, p. 015, 2013.

[10] T. Kaschub, A.-G. Paetz, P. Jochem, and W. Fichtner, "Feasibility of battery switch stations for local emission free public transport," in *Proc. ENERDAY 7th Conf. Energy Economics Technol.*, Dresden, Germany, 2012.

[11] Y. Miao, Q. Jiang, and Y. Cao, "Battery switch station modeling and its economic evaluation in microgrid," in *Proc. IEEE Power Energy Soc. General Meeting*, 2012, pp. 1–7.

[12] M. Takagi, Y. Iwafune, K. Yamaji, H. Yamamoto, K. Okano, R. Hiwatari, and T. Ikeya, "Economic value of PV energy storage using batteries of battery-switch stations," *IEEE Trans. Sustain. Energy*, vol. 4, no. 1, pp. 164–173, 2013.

[13] C. Wang, J. Yang, N. Liu, and Y. Mao, "Study on siting and sizing of battery-switch station," in *Proc. 4th Int. Conf. Electric Utility Deregulation and Restructuring and Power Technol.*, 2011, pp. 657–662.

[14] C. McPherson, J. Richardson, O. McLennan, and G. Zippel, "Planning an electric vehicle battery-switch network for Australia," in *Proc. Australasian Transport Res. Forum*, 2011.

[15] A. Kuperman, U. Levy, J. Goren, A. Zafransky, and A. Savernin, "Battery charger for electric vehicle traction battery switch station," *IEEE Trans. Ind. Electron.*, vol. 60, no. 12, pp. 5391–5399, Dec. 2013.

[16] P. Lombardi, M. Heuer, and Z. Styczynski, "Battery switch station as storage system in an autonomous power system: Optimization issue," in *Proc. IEEE Power and Energy Soc. General Meet.*, 2010, pp. 1–6.

[17] J. Yang and Z. Yang, "Optimal scheduling of electric vehicle using dual decomposition," in *Proc. 26th Chin. Control and Decision Conf.*, 2014, pp. 2144–2149.

[18] R. Deng, Z. Yang, J. Chen, and M.-Y. Chow, "Load scheduling with price uncertainty and temporally-coupled constraints in smart grids," *IEEE Trans. Power Syst.*, vol. 29, no. 4, pp. 2823–2834, Nov. 2014.

[19] O. Ardakanian, S. Keshav, and C. Rosenberg, "Real-time distributed control for smart electric vehicle chargers: From a static to a dynamic study," *IEEE Trans. Smart Grid*, vol. 5, pp. 2295–2305, Sep. 2014.

[20] R. Deng, Z. Yang, J. Chen, N. Asr, and M.-Y. Chow, "Residential energy consumption scheduling: A coupled-constraint game approach," *IEEE Trans. Smart Grid*, vol. 5, pp. 1340–1350, May 2014.

[21] P. You and Z. Yang, "Efficient optimal scheduling of charging station with multiple electric vehicles via v2v," in *Proc. IEEE Int. Conf. Smart Grid Commun.*, Nov. 2014, pp. 716–721.

[22] N. Li and J. Marden, "Designing games for distributed optimization," *IEEE J. Sel. Topics Signal Process.*, vol. 7, no. 2, pp. 230–242, Apr. 2013.

[23] S. Hosseini, A. Chapman, and M. Mesbahi, "Online distributed optimization via dual averaging," in *Proc. IEEE 52nd Annu. Conf. Decision and Control*, Dec. 2013, pp. 1484–1489.

[24] B. Chai, J. Chen, Z. Yang, and Y. Zhang, "Demand response management with multiple utility companies: A two-level game approach," *IEEE Trans. Smart Grid*, vol. 5, pp. 722–731, Mar. 2014.

[25] M. Zhu and S. Martinez, "On distributed convex optimization under inequality and equality constraints," *IEEE Trans. Autom. Control*, vol. 57, no. 1, pp. 151–164, Jan. 2012.

[26] M. G. Vaya, G. Andersson, and S. Boyd, "Decentralized control of plug-in electric vehicles under driving uncertainty," in *Proc. IEEE PES Innovative Smart Grid Technol. Conf. Europe*, 2014, pp. 1–6.

[27] J. Rivera, P. Wolfrum, S. Hirche, C. Goebel, and H.-A. Jacobsen, "Alternating direction method of multipliers for decentralized electric vehicle charging control," in *Proc. IEEE 52nd Annu. Conf. Decision and Control*, 2013, pp. 6960–6965.

[28] Z. Yang, K. Long, P. You, and M.-Y. Chow, "Joint scheduling of large-scale appliances and batteries via distributed mixed optimization," *IEEE Trans. Power Syst.*, vol. 30, no. 3, pp. 2031–2040, Jul. 2015.

[29] Y. He, B. Venkatesh, and L. Guan, "Optimal scheduling for charging and discharging of electric vehicles," *IEEE Trans. Smart Grid*, vol. 3, no. 3, pp. 1095–1105, 2012.

[30] A. Trippe, R. Arunachala, T. Massier, A. Jossen, and T. Hamacher, "Charging optimization of battery electric vehicles including cycle battery aging," in *Proc. IEEE PES Innovative Smart Grid Technol. Conf. Europe*, Oct. 2014, pp. 1–6.

[31] D. P. Bertsekas, *Nonlinear Programming*. Belmont, MA, : Athena Scientific, 1999.

Pengcheng You (S'14) received the B.S. degree in electrical engineering from Zhejiang University, China, in 2013, when he also graduated from Chu Kochen Honors College. He is currently working toward the Ph.D. degree at the College of Control Science and Engineering.

He is a member of the Group of Networked Sensing and Control in the State Key Laboratory of Industrial Control Technology, Zhejiang University. His research interests include optimization and control in smart grid.
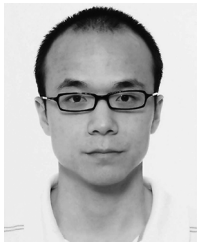
Zaiyue Yang (M'10) received the B.S. and M.S. degrees from the Department of Automation, University of Science and Technology of China, Hefei, China, in 2001 and 2004, respectively, and the Ph.D. degree from the Department of Mechanical Engineering, University of Hong Kong, in 2008.

Then, he was a Postdoctoral Fellow and Research Associate with the Department of Applied Mathematics, Hong Kong Polytechnic University before joining Zhejiang University, Hangzhou, China, in 2010. He is currently a Professor there. His current research interests include smart grid, signal processing and control theory.

Prof. Yang is an associate editor for the IEEE TRANSACTIONS ON INDUSTRIAL INFORMATICS.

Yongmin Zhang (S'12) received the Ph.D. degree in control science and engineering from Zhejiang University, Hangzhou, China.

He is currently a member of the Networked Sensing and Control Group and a Postdoctoral Research Fellow with the State Key Laboratory of Industrial Control Technology, Zhejiang University, Hangzhou, China. His research interests include wireless sensor networks and smart grid.
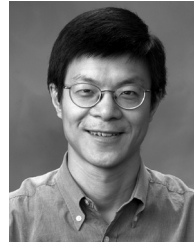
Steven H. Low (F'08) received the B.S. degree from Cornell University and the Ph.D. degree from the University of California, Berkeley, both in electrical engineering.

He is a Professor of the Department of Computing and Mathematical Sciences and the Department of Electrical Engineering at Caltech. Before that, he was with AT&T Bell Laboratories, Murray Hill, NJ, and the University of Melbourne, Australia.

Prof. Low was a corecipient of IEEE best paper awards and the R&D 100 Award. He is a senior editor of the IEEE TRANSACTIONS ON CONTROL OF NETWORK SYSTEMS and the IEEE TRANSACTIONS ON NETWORK SCIENCE AND ENGINEERING, is on the editorial boards of *NOW Foundations* and *Trends in Electric Energy Systems and in Networking*, as well as *Journal on Sustainable Energy, Grids and Networks*.

Youxian Sun received the Diploma from the Department of Chemical Engineering, Zhejiang University, China, in 1964.

He joined the Department of Chemical Engineering, Zhejiang University, in 1964. From 1984 to 1987, he was an Alexander Von Humboldt Research Fellow and Visiting Associate Professor at University of Stuttgart, Germany. He has been a Full Professor with Zhejiang University since 1988. In 1995, he was elevated to an Academician of the Chinese Academy of Engineering. His current research interests include modeling, control, and optimization of complex systems, and robust control design and its application. He is an IFAC Fellow and has authored/coauthored over 450 journal and conference papers. He is currently the Director of the Institute of Industrial Process Control and the National Engineering Research Center of Industrial Automation, Zhejiang University.

Prof. Sun is President of the Chinese Association of Automation and has served as Vice-Chairman of IFAC Pulp and Paper Committee and Vice-President of China Instrument and Control Society.